

# Correlated two-photon scattering in a 1D waveguide coupled to two- or three-level giant atoms

Wenju Gu,\* He Huang, Zhen Yi, Lei Chen, and Lihui Sun

*School of Physics and Optoelectronic Engineering, Yangtze University, Jingzhou 434023, China*

Huatang Tan†

*Department of Physics, Huazhong Normal University, Wuhan 430079, China*

(Dated: June 27, 2023)

We study the two-photon scattering processes in a one-dimensional (1D) waveguide coupled to a two- or three-level giant atom, respectively. The accumulated phase shift between the two coupling points can be utilized to alter the scattering processes. We obtain the exact interacting two-photon scattering wavefunction of these two systems following the Lippmann-Schwinger (LS) formalism, from which the analytical expressions of incoherent power spectra and second-order correlations are also derived. The incoherent spectrum, defined by the correlation of the bound state, serves as a useful indication of photon-photon correlation. The second-order correlation function gives a direct measure of photon-photon correlation. For photons scattered by the two-level giant atom, the accumulated phase shift can be used to improve photon-photon correlation, and adjust the evolution of the second-order correlation. In the system of the three-level giant atom, the photon-photon correlation can be substantially increased. Moreover, the photon-photon interactions and correlation distance of scattered photons can be further enhanced by tuning the accumulated phase shift.

## I. INTRODUCTION

Exploiting atom-photon interactions plays a critical role in the emerging field of waveguide quantum electrodynamics (QED) [1–4], which opens up novel opportunities both for fundamental physics [5–7] and for quantum information processing [8–10]. The conventional atom-photon interaction has been studied within the small atom regime, where the interaction is local because atoms are located in a region much smaller than the photon wavelength. Recently, a new paradigm referred to giant atoms, which support nonlocal couplings, is extensively investigated. This has been demonstrated by coupling artificial atoms to propagating fields (such as surface acoustic waves) whose wavelengths are smaller than the atomic sizes [11], or meandering waveguides at separated points [12, 13]. Due to nonlocal interactions, the self-interference between different atom-waveguide coupling points gives rise to a series of striking phenomena that are unachievable for small atoms, such as frequency-dependent Lamb shifts and relaxation rates [14], waveguide-mediated decoherence-free subspace [15, 16], nonexponential decay [11, 17, 18], and oscillating bound states [19].

Waveguide QED systems usually allow for a one-dimensional (1D) continuum of modes, lowering the restrictions on the bandwidth of the fields, while also achieving strong coupling to local emitters by reducing the mode volume [1]. Few-photon scattering is well studied in the strong-coupling regime, where the

light-matter interaction dominates over loss and dephasing. A variety of theoretical techniques have been developed to studying few-photon scattering within the small atom regime. These techniques include the real-space Bethe-ansatz method [20, 21], the Lehmann-Symanzik-Zimmermann reduction [22, 23], the wave-packet evolution approach [24, 25], the Lippmann-Schwinger (LS) formalism [26, 27], input-output formalism [28, 29], as well as the Dyson series summation [30].

Currently, photon scattering in giant-atom waveguide QED systems has attracted a lot of attention due to the unique interference effect [31–34]. To our knowledge, the majority of studies focus on the single-photon level, while the few-photon scattering within the giant atom regime is less investigated. The nonlinearity of atomic system would induce photon-photon correlations, while photon-photon correlations induced tunneling or blocking of photons would affect transmission and reflection of photons [35–38]. Therefore, a clear understanding of the nature of photon-photon correlations is crucial to figure out how various quantum devices work, such as a switchable mirror [39] or a single-photon router [40]. The few-photon scattering wavefunctions exhibit a common structure: the two-particle plane wave with momenta of photons rearranged and bound state. The plane wave originates from the coherent scattering, and the bound state originates from the incoherent scattering. The bound state decays exponentially as the distance between two photons increases, and also refers to the two-particle irreducible T-matrix in scattering theory [41].

In this work, we employ the LS formalism to treat the two-photon scattering processes of two- and three-level giant atom coupled to a 1D waveguide, respectively. It is able to obtain the exact two-photon interacting scattering wavefunction of two systems. Furthermore, the inco-

\* guwenju@yangtzeu.edu.cn; School of Physics and Optoelectronic Engineering, Yangtze University, Jingzhou 434023, China

† tht@mail.ccnu.edu.cn

herent power spectrum is derived from the correlation of the bound state, and its total flux provides a indication of photon-photon correlation. The second-order correlation function gives a direct measure of photon-photon correlation. Based on these solutions, we find that the accumulated phase shift can be used to improve photon-photon correlation, and adjust the evolution of the second-order correlation for photons scattered by the two-level giant atom. In comparison to the two-level giant atom, the photon-photon correlation can be substantially increased for the system of the three-level giant atom. The photon-photon interactions can be further improved and the decay distance of second-order correlation can be increased by tuning the accumulated phase shift between the two coupling points.

The paper is organized as follows. In Sec. II and III, we study the two-photon scattering in the system of the two-level giant atom and the three-level giant atom coupled to a 1D waveguide, respectively, including the two-photon interacting scattering eigenstate, the incoherent power spectrum and second-order correlation functions. The conclusion is given in Sec. IV. A summary of technical details that are relevant to the incoherent power spectrum in Appendix.

## II. THE SYSTEM OF A TWO-LEVEL GIANT ATOM COUPLED TO A 1D WAVEGUIDE

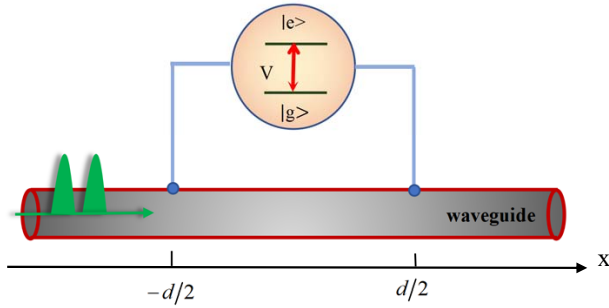


FIG. 1. Schematic illustration of a two-level giant atom sidely coupled to a one-dimensional (1D) waveguide. The atomic transition  $|g\rangle \leftrightarrow |e\rangle$  is coupled to waveguide modes at the points of  $x = -d/2$  and  $x = d/2$ , respectively, with strength  $V$ .

We begin by considering correlated two-photon dynamics in the system consisting of a two-level giant atom sidely coupled to a 1D waveguide, as shown in Fig. 1. The atomic transition  $|g\rangle \leftrightarrow |e\rangle$  interacts with the waveguide field at the coupling points of  $x = -d/2$  and  $x = d/2$ , respectively. The single-photon scattering process has been considered in Ref. [42]. Here we focus on the two-photon dynamics to explore photon-photon interactions. The Hamiltonian of the system can written as ( $\hbar = 1$

hereafter)

$$\begin{aligned} \hat{H} = & (\omega_0 - i\gamma_e/2) \hat{\sigma}_{ee} \\ & - i\nu_g \int dx \left[ \hat{a}_R^\dagger(x) \partial_x \hat{a}_R(x) - \hat{a}_L^\dagger(x) \partial_x \hat{a}_L(x) \right] \\ & + \frac{V}{2} \sum_{\alpha=R,L} \int dx M(x) [\hat{a}_\alpha^\dagger(x) \hat{\sigma}^- + \hat{\sigma}^+ \hat{a}_\alpha(x)]. \end{aligned} \quad (1)$$

Here  $M(x) = \delta(x + d/2) + \delta(x - d/2)$  denotes the coupling points,  $\hat{a}_R^\dagger(x)$  and  $\hat{a}_L^\dagger(x)$  are the creation operators for the right-moving and left-moving modes in real space, and  $\nu_g$  is the group velocity. We will take  $\nu_g = 1$  for simplicity. For the two-level giant atom,  $\omega_0$  is the atomic transition frequency, and  $\gamma_e$  is the spontaneous emission rate of the excited state to modes other than the waveguide continuum. The atomic transition  $|g\rangle \leftrightarrow |e\rangle$  couples to the waveguide modes at  $x = -d/2$  and  $x = d/2$  with the same strength  $V = \sqrt{2\Gamma}$ , where  $\Gamma$  is the atomic spontaneous decay rate to the waveguide continuum. In the strong coupling limit, the Purcell factor  $P$  is large, i.e.,  $P = \Gamma/\gamma_e \gg 1$ . For instance,  $\Gamma/2\pi = 2\text{MHz}$  and  $\gamma_e/2\pi = 0.03\text{MHz}$  are demonstrated in the experimental setup [12]. This indicates that the spontaneous decay is mainly to the waveguide compared with all the other modes. In this case, the atomic spontaneous dissipation rate  $\gamma_e$  can be ignored.

The total excitation number is conserved for the Jaynes-Cummings model of interactions between the atom and waveguide field. Thus, in the single-excitation subspace, the eigenstate of the system can be written in the form

$$\begin{aligned} |\phi_1(k)\rangle_\alpha = & \int dx \left[ \phi_R^\alpha(k, x) \hat{a}_R^\dagger(x) + \phi_L^\alpha(k, x) \hat{a}_L^\dagger(x) \right] |0, g\rangle \\ & + u_e^\alpha(k) |0, e\rangle, \end{aligned} \quad (2)$$

where  $\alpha = \{R, L\}$ , and  $\phi_{R/L}^\alpha(k, x)$  denote the probability amplitudes of creating the right-moving and left-moving photons in real space for the  $\alpha$ -direction incident photon with wavevector  $k$ , respectively.  $u_e^\alpha(k)$  is the excitation amplitude of the atom, and  $|0, g\rangle$  denotes the vacuum state of the system. The probability amplitudes can be determined by the Schrödinger equation  $\hat{H} |\phi_1(k)\rangle_\alpha = k |\phi_1(k)\rangle_\alpha$ , which gives

$$\begin{aligned} (\omega_0 - k) u_e^\alpha(k) + \sqrt{\frac{\Gamma}{2}} \int dx M(x) [\phi_R^\alpha(k, x) + \phi_L^\alpha(k, x)] &= 0, \\ (-i\partial_x - k) \phi_R^\alpha(k, x) + \sqrt{\frac{\Gamma}{2}} M(x) u_e^\alpha(k) &= 0, \\ (i\partial_x - k) \phi_L^\alpha(k, x) + \sqrt{\frac{\Gamma}{2}} M(x) u_e^\alpha(k) &= 0. \end{aligned} \quad (3)$$

The solution of wavefunction takes the following form

$$\begin{aligned}
\phi_R^R(k, x) &= \frac{e^{ikx}}{\sqrt{2\pi}} \left\{ \theta(-d/2 - x) + t_1(k) [\theta(x + d/2) \right. \\
&\quad \left. - \theta(x - d/2)] + t_2(k) \theta(x - d/2) \right\}, \\
\phi_L^R(k, x) &= \frac{e^{-ikx}}{\sqrt{2\pi}} \left\{ r_1(k) \theta(-d/2 - x) \right. \\
&\quad \left. + r_2(k) [\theta(x + d/2) - \theta(x - d/2)] \right\}, \\
\phi_R^L(k, x) &= \frac{e^{ikx}}{\sqrt{2\pi}} \left\{ r_1(k) \theta(x - d/2) \right. \\
&\quad \left. + r_2(k) [\theta(x + d/2) - \theta(x - d/2)] \right\}, \\
\phi_L^L(k, x) &= \frac{e^{-ikx}}{\sqrt{2\pi}} \left\{ \theta(x - d/2) + t_1(k) [\theta(x + d/2) \right. \\
&\quad \left. - \theta(x - d/2)] + t_2(k) \theta(-d/2 - x) \right\}, \quad (4)
\end{aligned}$$

where  $\theta(x)$  is the Heaviside step function. Here,  $t_2(k)$  and  $r_1(k)$  denote the single-photon transmission and reflection amplitudes in the regions of  $x > d/2$  and  $x < -d/2$ , respectively, and  $t_1(k)$  and  $r_2(k)$  are the probability amplitudes for the transmission and reflection between the two coupling points  $-d/2 < x < d/2$ . These amplitudes are

$$\begin{aligned}
t_1(k) &= \frac{\omega_0 - k - i\Gamma/2 (1 + e^{ikd})}{\omega_0 - k - i\Gamma (1 + e^{ikd})}, \\
t_2(k) &= \frac{\omega_0 - k + \Gamma \sin kd}{\omega_0 - k - i\Gamma (1 + e^{ikd})}, \\
r_1(k) &= \frac{i\Gamma (1 + \cos kd)}{\omega_0 - k - i\Gamma (1 + e^{ikd})}, \\
r_2(k) &= \frac{i\Gamma/2 (1 + e^{ikd})}{\omega_0 - k - i\Gamma (1 + e^{ikd})}, \\
u_e^\alpha(k) &= \frac{-\sqrt{\Gamma/\pi} \cos(kd/2)}{\omega_0 - k - i\Gamma (1 + e^{ikd})}. \quad (5)
\end{aligned}$$

In order to study two-photon scattering processes, we employ the the LS equation to obtain the two-photon scattering eigenstate [26, 27]. Because of nonlinear effects of the two-level atom, it is practical to use a bosonic representation which involves an on-site interaction [26, 43],

$$H = H_0 + V, \quad V = \frac{U}{2} \hat{d}^\dagger \hat{d} (\hat{d}^\dagger \hat{d} - 1). \quad (6)$$

The atomic operators  $\hat{\sigma}^\pm$  in  $\hat{H}_0$  are replaced by the bosonic creation and annihilation operators  $\hat{d}^\dagger$  and  $\hat{d}$ , respectively. To map the atomic ground and excited states to zero- and one-boson states,  $U \rightarrow \infty$  should be taken in the end to project out occupations greater than 1. In this bosonic representation, it corresponds to a non-interacting Hamiltonian if  $U = 0$  and can readily

be solved. The non-interacting two-photon eigenstate is

$$|\phi_2(k_1, k_2)\rangle_{\alpha_1 \alpha_2} = \frac{1}{\sqrt{2}} |\phi_1(k_1)\rangle_{\alpha_1} \otimes |\phi_1(k_2)\rangle_{\alpha_2}. \quad (7)$$

The LS equation provides the relationship between the full interacting two-photon eigenstates  $|\psi_2(k_1, k_2)\rangle_{\alpha_1 \alpha_2}$  and  $|\phi_2(k_1, k_2)\rangle_{\alpha_1 \alpha_2}$  as

$$|\psi_2(k_1, k_2)\rangle_{\alpha_1 \alpha_2} = |\phi_2(k_1, k_2)\rangle_{\alpha_1 \alpha_2} + G^R(E) V |\psi_2(k_1, k_2)\rangle_{\alpha_1 \alpha_2}, \quad (8)$$

where  $G^R(E) = 1/(E - H_0 + i0^+)$  is the retarded Green function, and  $E$  is the total energy of the two incident photons. The two-particle identity operator in real space can be written as

$$\begin{aligned}
I_2 &= I_2^x \otimes |0\rangle \langle 0| + I_1^x \otimes |d\rangle \langle d| + I_0^x \otimes |dd\rangle \langle dd|, \\
I_n^x &= \sum_{\alpha_1 \dots \alpha_n = R, L} \int \dots \int dx_1 \dots dx_n |x_1 \dots x_n\rangle_{\alpha_1 \dots \alpha_n} \langle x_1 \dots x_n|, \quad (9)
\end{aligned}$$

where  $|0\rangle$  is the ground state, and we denote the single-excitation state  $|d\rangle = \hat{d}^\dagger |0\rangle$  and two-excitation state  $|dd\rangle = \hat{d}^{\dagger 2} |0\rangle / \sqrt{2}$ . Via inserting the identity operator into Eq. (8) we have

$$\begin{aligned}
&|\psi_2(k_1, k_2)\rangle_{\alpha_1 \alpha_2} \\
&= |\phi_2(k_1, k_2)\rangle_{\alpha_1 \alpha_2} + G^R(E) V I_2 |\psi_2(k_1, k_2)\rangle_{\alpha_1 \alpha_2} \\
&= |\phi_2(k_1, k_2)\rangle_{\alpha_1 \alpha_2} + U G^R(E) |dd\rangle \langle dd| |\psi_2(k_1, k_2)\rangle_{\alpha_1 \alpha_2}. \quad (10)
\end{aligned}$$

Firstly, by projecting Eq. (10) onto  $\langle dd|$ ,

$$\langle dd | \psi_2(k_1, k_2) \rangle_{\alpha_1 \alpha_2} = (1 - U G_{dd})^{-1} \langle dd | \phi_2(k_1, k_2) \rangle_{\alpha_1 \alpha_2}, \quad (11)$$

where  $G_{dd} = \langle dd | G^R(E) | dd \rangle$ . Then projecting Eq. (10) onto a two-photon basis state  $_{\alpha'_1 \alpha'_2} \langle x_1 x_2 |$  and taking the  $U \rightarrow \infty$  limit, the interacting two-photon eigenstate eventually becomes

$$\begin{aligned}
_{\alpha'_1 \alpha'_2} \langle x_1 x_2 | \psi_2(k_1, k_2) \rangle_{\alpha_1 \alpha_2} &= _{\alpha'_1 \alpha'_2} \langle x_1 x_2 | \phi_2(k_1, k_2) \rangle_{\alpha_1 \alpha_2} \\
&\quad - C_{xd}^{\alpha'_1 \alpha'_2} (x_1, x_2) G_{dd}^{-1} \langle dd | \phi_2(k_1, k_2) \rangle_{\alpha_1 \alpha_2}, \quad (12)
\end{aligned}$$

where  $G_{xd}^{\alpha'_1 \alpha'_2} (x_1, x_2) = _{\alpha'_1 \alpha'_2} \langle x_1 x_2 | G^R(E) | dd \rangle$ , and  $x_1$  and  $x_2$  refer to the positions of the photons. The first term denotes the plane-wave state, while the second term contains all the nonlinearity and is usually referred to as the two-photon bound state. In order to solve the Green functions, we can use the two-photon non-interacting scattering eigenstates to establish a two-particle identity in momentum space

$$I'_2 = \sum_{\alpha_1, \alpha_2 = R, L} \iint dk_1 dk_2 |\phi_2(k_1, k_2)\rangle_{\alpha_1 \alpha_2} \langle \phi_2(k_1, k_2)|. \quad (13)$$

The Green functions can finally be obtained in the form

$$\begin{aligned}
G_{dd} &= \sum_{\alpha_1, \alpha_2 = R, L} \iint dk_1 dk_2 \frac{\langle dd | \phi_2(k_1, k_2) \rangle_{\alpha_1 \alpha_2} \langle \phi_2(k_1, k_2) | dd \rangle}{E - k_1 - k_2 + i0^+}, \\
G_{xd}^{\alpha_1 \alpha_2}(x_1, x_2) &= \sum_{\alpha'_1, \alpha'_2 = R, L} \iint dk_1 dk_2 \frac{\alpha_1 \alpha_2 \langle x_1 x_2 | \phi_2(k_1, k_2) \rangle_{\alpha'_1 \alpha'_2} \langle \phi_2(k_1, k_2) | dd \rangle}{E - k_1 - k_2 + i0^+},
\end{aligned} \tag{14}$$

with the elements

$$\begin{aligned}
\langle dd | \phi_2(k_1, k_2) \rangle_{\alpha_1 \alpha_2} &= u_e^{\alpha_1}(k_1) u_e^{\alpha_2}(k_2), \\
\alpha'_1 \alpha'_2 \langle x_1 x_2 | \phi_2(k_1, k_2) \rangle_{\alpha_1 \alpha_2} &= \frac{1}{2} \left( \phi_{\alpha'_1}^{\alpha_1}(k_1, x_1) \phi_{\alpha'_2}^{\alpha_2}(k_2, x_2) \right. \\
&\quad \left. + \phi_{\alpha'_1}^{\alpha_2}(k_2, x_1) \phi_{\alpha'_2}^{\alpha_1}(k_1, x_2) \right).
\end{aligned} \tag{15}$$

When the propagating time of photons between the coupling points is shorter than the atomic lifetime  $1/\Gamma$ , the Markovian approximation is feasible. Hence, the wavevector  $k$  in the phase factors can be replaced by a constant  $k_0 = \omega_0/\nu_g$ , and the accumulated phase shift between the coupling points is denoted by  $\vartheta = k_0 d$ . In principle, the phase shift can be adjusted by changing the distance of the coupling points. Then, via taking the double integral with the use of standard contour integral techniques, the Green functions become

$$\begin{aligned}
G_{dd} &= \frac{1}{E - 2\omega_0 + i2\Gamma'}, \\
G_{xd}^{RR}(x_1, x_2) &= \frac{-\Gamma(1 + \cos \vartheta)}{E - 2\omega_0 + i2\Gamma'} e^{iEx_c} e^{i(E/2 - \omega_0)|x| - \Gamma'|x|},
\end{aligned} \tag{16}$$

where  $\Gamma' = \Gamma(1 + e^{i\vartheta})$ . During the contour integrations,  $x_1 > d/2$ ,  $x_2 > d/2$ , and  $x = x_2 - x_1$ ,  $x_c = (x_1 + x_2)/2$  are used. It can be proved that  $G_{xd}^{LL}(-x_1, -x_2) = G_{xd}^{RR}(x_1, x_2) = G_{xd}^{RL}(x_1, -x_2) = G_{xd}^{LR}(-x_1, x_2)$  because of the parity symmetry. By substituting these expressions to Eq. (12), the interacting two-photon eigenstate is

$$\begin{aligned}
|\psi_2(k_1, k_2)\rangle_{RR} &= \\
&\iint dx_1 dx_2 f_{RR}(x_1, x_2) \frac{1}{\sqrt{2}} \hat{a}_R^\dagger(x_1) \hat{a}_R^\dagger(x_2) |0\rangle \\
&+ \iint dx_1 dx_2 f_{LL}(x_1, x_2) \frac{1}{\sqrt{2}} \hat{a}_L^\dagger(x_1) \hat{a}_L^\dagger(x_2) |0\rangle \\
&+ \iint dx_1 dx_2 f_{RL}(x_1, x_2) \hat{a}_R^\dagger(x_1) \hat{a}_L^\dagger(x_2) |0\rangle.
\end{aligned} \tag{17}$$

The coefficients are

$$\begin{aligned}
f_{RR}(x_1, x_2) &= e^{iEx_c} \frac{\sqrt{2}}{2\pi} [t_2(k_1) t_2(k_2) \cos \Delta_1 x + B_{k_1, k_2}(x)], \\
f_{LL}(x_1, x_2) &= e^{-iEx_c} \frac{\sqrt{2}}{2\pi} [r_1(k_1) r_1(k_2) \cos \Delta_1 x + B_{k_1, k_2}(x)], \\
f_{RL}(x_1, x_2) &= \frac{e^{iEx/2}}{2\pi} \left[ t_2(k_1) r_1(k_2) e^{2i\Delta_1 x_c} \right. \\
&\quad \left. + r_1(k_1) t_2(k_2) e^{-2i\Delta_1 x_c} + 2B_{k_1, k_2}(x_c) \right], \\
B_{k_1, k_2}(x) &= \frac{\Gamma^2(1 + \cos \vartheta)^2}{(E/2 - \omega_0 + i\Gamma')^2 - \Delta_1^2} e^{i(E/2 - \omega_0)|x| - \Gamma'|x|},
\end{aligned} \tag{18}$$

where  $\Delta_1 = (k_1 - k_2)/2$  corresponds to half of the energy difference between the two incident photons. For the case of  $\vartheta = 0$ , the interacting eigenstate can be simplified to the same form as that of the small two-level atom scenario with the single coupling point in Ref. [44] by replacing  $\Gamma$  with  $\Gamma/4$ . The factor 4 comes from the constructive interference between the two coupling points.

For the input of two-particle plane wave, scattering wavefunctions exhibit a common constituent: the two-particle plane wave with momenta of photons rearranged and the bound state. The plane wave originates from the coherent scattering, while the bound state originates from the incoherent scattering. It decays exponentially with the increasing of the distance between two photons, and also refers to the two-particle irreducible T-matrix in scattering theory [41].

## A. Incoherent power spectrum and second-order correlation function

### 1. Incoherent power spectrum

The interacting two-photon eigenstate contains two contributions: the plane wave originated from coherent scattering, and the bound state originated from photon-photon interactions. To investigate the effects on scattering processes, we first consider the power spectrum or resonance fluorescence, which is the Fourier transform of the first-order correlation function,

$$S_\alpha(\omega) = \int dt e^{-i\omega t} \langle \psi_2 | \hat{a}_\alpha^\dagger(x_0) \hat{a}_\alpha^\dagger(x_0 + t) | \psi_2 \rangle, (\alpha = R, L), \tag{19}$$

where  $x_0$  is the position of the detector that is far away from the scattering region.  $S_\alpha(\omega)$  accounts for the spectral decomposition of the photons in the interacting two-photon wavefunction  $|\psi_2\rangle$ . The detailed derivation of power spectrum is presented in the Appendix A. In general, the power spectrum consists of the coherent and incoherent parts, i.e.,  $S_\alpha(\omega) = S_\alpha^{\text{coherent}}(\omega) + S_\alpha^{\text{incoherent}}(\omega)$ . The coherent scattering gives a  $\delta$ -function contribution, and incoherent scattering is given by the correlation of the bound state of the wavefunction, as shown in Eq. (A5). The total incoherent power spectrum, which is defined by

$$F(k) = \sum_{\alpha=R,L} \int d\omega S_\alpha^{\text{incoherent}}(\omega), \quad (20)$$

can provide a measure of the overall strength of correlations. Under the condition of identical incident photons:  $k_1 = k_2 = k = E/2$ ,

$$F(k) = \frac{4\Gamma^3(1 + \cos\vartheta)^3}{\pi |E/2 - \omega_0 + i\Gamma'|^4}, \quad (21)$$

which is consistent with that of the single coupling point (by replacing  $\Gamma$  with  $\Gamma/4$ ) for the case of  $\vartheta = 0$  [45].

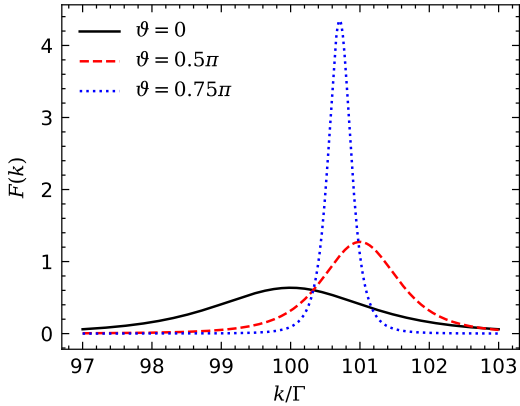


FIG. 2. The total incoherent power spectrum  $F(k)$  as a function of the incident frequency  $k$  with different values of accumulated phase shift  $\vartheta$ . The other parameters are  $\omega_0 = 100\Gamma$  and  $k_1 = k_2 = k = E/2$ .

The total incoherent power spectrum  $F(k)$  as a function of the incident frequency  $k$  is presented in Fig. 2. The large value of  $F(k)$  indicates that there will be strong correlation effects, since the incoherent scattering originates from the correlation of bound state. Therefore, the peak value of  $F(k)$  corresponds to the strongest correlation, and  $k_{\text{peak}}$  is the best incident frequency to obtain photon-photon correlations. It also shows that the values of  $F_{\text{peak}}$  and  $k_{\text{peak}}$  vary with the phase shift  $\vartheta$ . For example, when  $\vartheta = 0.75\pi$ ,  $F_{\text{peak}}$  can reach about seven times larger than that of  $\vartheta = 0$ , which suggests substantially enhanced photon-photon correlations. Physically, the position and the width of the peak can be

explained by the pole of the system, which is the zero of the denominator of the single-photon transmission or reflection amplitude  $t(k)$  or  $r(k)$ . If we denote the pole by  $z = \tilde{\omega} - i\tilde{\Gamma}$ , where the real part  $\tilde{\omega} = \omega_0 + \Gamma \sin \theta$  is the eigenfrequency and  $\tilde{\Gamma} = \Gamma(1 + \cos \theta)$  is the effective decay rate. The position of peak corresponds to the eigenfrequency  $\tilde{\omega}$  and the width is  $\tilde{\Gamma}$ . The corresponding peak value is  $F_{\text{peak}} = 4/\pi\tilde{\Gamma}$ . Compared to the single coupling point of small atom, the peak value is  $8/\pi\Gamma$ , which can be surpassed in the giant atom with  $\vartheta \in (2\pi/3, 5\pi/3)$ . Thus, the small value of the effective decay rate can promote photon-photon correlations, and it is tunable with the change of phase shift  $\vartheta$  in the two-level giant atom system.

## B. Second-order correlation function

Next, we employ the second-order correlation function to investigate the photon-photon correlation [46]. The second-order correlation function of the transmitted field ( $x_1 > d/2$ ,  $x_2 > d/2$  and  $x = x_2 - x_1$ ) is defined by

$$g_R^{(2)}(x) = \frac{\langle \psi_2 | \hat{a}_R^\dagger(x_1) \hat{a}_R^\dagger(x_2) \hat{a}_R(x_2) \hat{a}_R(x_1) | \psi_2 \rangle}{\langle \psi_2 | \hat{a}_R^\dagger(x_1) \hat{a}_R(x_1) | \psi_2 \rangle^2}. \quad (22)$$

For the weak incident coherent state (mean photon number  $\bar{n} \ll 1$  of right-moving photons is assumed),  $g_R^{(2)}(x)$  can be approximately equal to

$$\begin{aligned} g_R^{(2)}(x) &\approx \frac{|_{RR} \langle x_1 x_2 | \psi_2(k_1, k_2) \rangle_{RR}|^2}{|_R \langle x_1 | \phi_1(k_1) \rangle_R|^2 |_R \langle x_2 | \phi_1(k_2) \rangle_R|^2} \\ &= \frac{2\pi^2 |f_{RR}(x_1, x_2)|^2}{|t_2(k_1)|^2 |t_2(k_2)|^2}. \end{aligned} \quad (23)$$

Likewise, the second-order correlation function of the reflected photons is

$$\begin{aligned} g_L^{(2)}(x) &= \frac{|_{LL} \langle x_1 x_2 | \psi_2(k_1, k_2) \rangle_{RR}|^2}{|_L \langle x_1 | \phi_1(k_1) \rangle_R|^2 |_L \langle x_2 | \phi_1(k_2) \rangle_R|^2} \\ &= \frac{2\pi^2 |f_{LL}(x_1, x_2)|^2}{|r_1(k_1)|^2 |r_1(k_2)|^2}. \end{aligned} \quad (24)$$

Also for the identical incident photons:  $k_2 = k_2 = E/2$  and by substituting the explicit expressions, the second-order correlation functions can be simplified as

$$\begin{aligned} g_R^{(2)}(x) &= \left| 1 + \frac{\Gamma^2(1 + \cos\vartheta)^2}{(E/2 - \omega_0 - \Gamma \sin\vartheta)^2} e^{i(E/2 - \omega_0)|x| - \Gamma'|x|} \right|^2, \\ g_L^{(2)}(x) &= \left| 1 - e^{i(E/2 - \omega_0)|x| - \Gamma'|x|} \right|^2, \end{aligned} \quad (25)$$

which are numerically plotted in Fig. 3. For  $\vartheta = 0$ , the behavior of  $g_{R/L}^{(2)}(x)$  resembles that of the single coupling point, which has been extensively investigated in theory as well as experiment with microwave photons [40].

The transmitted photons are bunched while the reflected photons are anti-bunched. The correlations reach to 1 quickly with little structure. Consequently, the initial value  $g_R^{(2)}(0)$  makes a good prediction of the nature of the correlation overall. In physics,  $g_L^{(2)}(0) = 0$  of the reflected field is due to the two-level atom can only absorb and emit one photon at a time [40].

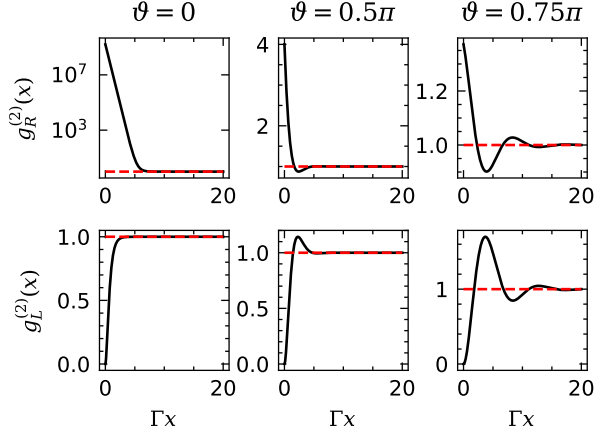


FIG. 3. Second-order correlation functions  $g_R^{(2)}(x)$  (transmitted photons, first row) and  $g_L^{(2)}(x)$  (reflected photons, second row) as a function of  $x$ . First column is  $\vartheta = 0$ , second column is  $\vartheta = 0.5\pi$ , and third column is  $\vartheta = 0.75\pi$ . The dashed horizontal line refers to  $g^{(2)}(x) = 1$ . The other parameters are  $\omega_0 = 100\Gamma$ ,  $k_1 = k_2 = E/2 = \omega_0$ .

However, for  $\vartheta = 0.5\pi$  and  $\vartheta = 0.75\pi$ ,  $g_{R/L}^{(2)}(x)$  exhibit an oscillation between bunching and anti-bunching, and take a longer time to reach 1. Such a behavior reveals that photons become organized periodically in time and space. Since the oscillation is appeared in  $g_{R/L}^{(2)}(x)$ , the initial correlation  $g_{R/L}^{(2)}(0)$  cannot serve as a prediction of whether the system generates bunching or anti-bunching of photons. These features can be also explained by the pole of the system, which is appeared in the exponential factor of Eq. (25). Then, the presence of oscillation results from beating between the eigenfrequency and the driving frequency, and its duration is determined by the effective decay rate. Therefore, for  $\vartheta = 0$ , the effective decay rate takes the maximum value  $2\Gamma$  and  $g_{R/L}^{(2)}(x)$  reach to 1 rapidly. For  $\vartheta = 0.5\pi$ , the effective decay rate equals to  $\Gamma$ , and the oscillation extends for a long time. For  $\vartheta = 0.75\pi$ , the effective decay rate becomes smaller and the oscillation extends for a longer time.

### III. THE SYSTEM OF A THREE-LEVEL GIANT ATOM COUPLED TO A 1D WAVEGUIDE

We further consider correlated two-photon dynamics in the system consisting of a 1D waveguide sidely coupled to a three-level  $\Lambda$ -type giant atom as shown in Fig. 4.

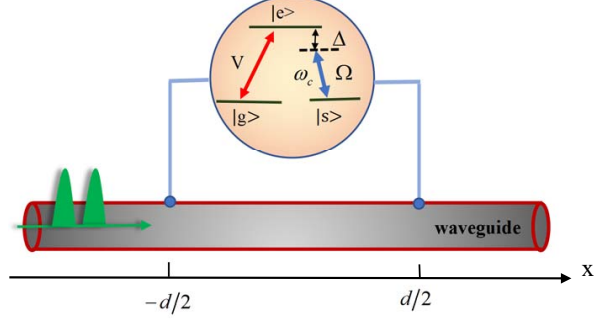


FIG. 4. Schematic illustration of a three-level giant atom sidely coupled to a 1D waveguide. The transition  $|g\rangle \leftrightarrow |e\rangle$  is coupled to waveguide modes with strength  $V$  at  $x = -d/2$  and  $x = d/2$ . The transition  $|e\rangle \leftrightarrow |s\rangle$  is driven by a laser field of frequency  $\omega_c$  with Rabi frequency  $\Omega$ , and the detuning is  $\Delta$ .

For the single coupling point, it shows that the second-order correlation of the scattered photons can be tuned by changing Rabi frequency of the control beam [47]. Now, our attention is specifically focused on how the accumulated phase shift affects non-classical properties of scattered fields. The system is described by the Hamiltonian ( $\hbar = 1$  and the group velocity  $\nu_g = 1$ )

$$\begin{aligned} \hat{H} = & -i \int dx \left[ \hat{a}_R^\dagger(x) \partial_x \hat{a}(x) - \hat{a}_L^\dagger(x) \partial_x \hat{a}_L(x) \right] \\ & + (\omega_0 - i\gamma_e/2) \hat{\sigma}_{ee} + (\omega_0 - \Delta) \hat{\sigma}_{ss} + \frac{\Omega}{2} (\hat{\sigma}_{es} + \hat{\sigma}_{se}) \\ & + \frac{V}{2} \sum_{\alpha=R,L} \int dx M(x) \left[ \hat{a}_\alpha^\dagger(x) \hat{\sigma}_{ge} + \hat{\sigma}_{eg} \hat{a}_\alpha(x) \right], \end{aligned} \quad (26)$$

where  $M(x) = \delta(x + d/2) + \delta(x - d/2)$  denotes positions of coupling points,  $\omega_0$  is the transition frequency of  $|g\rangle \rightarrow |e\rangle$ , and  $\Delta$  denotes the detuning between the transition frequency  $|s\rangle \rightarrow |e\rangle$  and the laser driving frequency  $\omega_c$ . Also, in the strong atom-waveguide coupling regime that is realizable in experimental setups, i.e.,  $\Gamma = V^2/2 \gg \gamma_e$ , the atomic spontaneous dissipation rate  $\gamma_e$  can be ignored. The eigenstate of the system in the single-excitation subspace can be written in the form

$$\begin{aligned} |\phi_1(k)\rangle_\alpha = & \int dx \left[ \phi_R^\alpha(k, x) \hat{a}_R^\dagger(x) + \phi_L^\alpha(k, x) \hat{a}_L^\dagger(x) \right] |0, g\rangle \\ & + u_e^\alpha(k) |0, e\rangle + u_s^\alpha(k) |0, s\rangle. \end{aligned} \quad (27)$$

Here  $\phi_{R/L}^\alpha(k, x)$  indicate the probability amplitudes of creating the right-moving and left-moving photons in real space for the  $\alpha$ -direction incoming photon with wavevector  $k$ , respectively;  $u_e^\alpha(k)$  is the excitation amplitude of the atomic level  $|e\rangle$ ;  $u_s^\alpha(k)$  is the excitation amplitude of the atomic level  $|s\rangle$ . These probability amplitudes can be determined by the Schrödinger equation

$\hat{H} |\phi_1(k)\rangle_\alpha = k |\phi_1(k)\rangle_\alpha$ , which obey

$$\begin{aligned} -i\partial_x\phi_R^\alpha(k, x) + \sqrt{\frac{\Gamma}{2}}M(x)u_e^\alpha(k) &= k\phi_R^\alpha(k, x), \\ i\partial_x\phi_L^\alpha(k, x) + \sqrt{\frac{\Gamma}{2}}M(x)u_e^\alpha(k) &= k\phi_L^\alpha(k, x), \\ \omega_0 u_e^\alpha(k) + \frac{\Omega}{2}u_s^\alpha(k) + \sqrt{\frac{\Gamma}{2}}\sum_{\alpha'=R, L}\int dx M(x)\phi_{\alpha'}^\alpha(k, x) \\ &= ku_e^\alpha(k), \\ (\omega_0 - \Delta)u_s^\alpha(k) + \frac{\Omega}{2}u_e^\alpha(k) &= ku_s^\alpha(k). \end{aligned} \quad (28)$$

The solutions of wavefunction take the following form

$$\begin{aligned} \phi_R^R(k, x) &= \frac{e^{ikx}}{\sqrt{2\pi}}\{\theta(-d/2 - x) + t_1(k)[\theta(x + d/2) \\ &\quad - \theta(x - d/2)] + t_2(k)\theta(x - d/2)\}, \\ \phi_L^R(k, x) &= \frac{e^{-ikx}}{\sqrt{2\pi}}\{r_1(k)\theta(-d/2 - x) \\ &\quad + r_2(k)[\theta(x + d/2) - \theta(x - d/2)]\}, \\ \phi_R^L(k, x) &= \frac{e^{ikx}}{\sqrt{2\pi}}\{r_1(k)\theta(x - d/2) \\ &\quad + r_2(k)[\theta(x + d/2) - \theta(x - d/2)]\}, \\ \phi_L^L(k, x) &= \frac{e^{-ikx}}{\sqrt{2\pi}}\{\theta(x - d/2) + t_1(k)[\theta(x + d/2) \\ &\quad - \theta(x - d/2)] + t_2(k)\theta(-d/2 - x)\}, \end{aligned} \quad (29)$$

where the coefficients are

$$\begin{aligned} t_1(k) &= \frac{(\omega_0 - \Delta - k)[\omega_0 - k - i\Gamma/2(1 + e^{ikd})] - \Omega^2/4}{(\omega_0 - \Delta - k)[\omega_0 - k - i\Gamma(1 + e^{ikd})] - \Omega^2/4}, \\ t_2(k) &= \frac{(\omega_0 - \Delta - k)(\omega_0 - k + \Gamma \sin kd) - \Omega^2/4}{(\omega_0 - \Delta - k)[\omega_0 - k - i\Gamma(1 + e^{ikd})] - \Omega^2/4}, \\ r_1(k) &= \frac{i\Gamma(\omega_0 - \Delta - k)(1 + \cos kd)}{(\omega_0 - \Delta - k)[\omega_0 - k - i\Gamma(1 + e^{ikd})] - \Omega^2/4}, \\ r_2(k) &= \frac{i\Gamma/2(\omega_0 - \Delta - k)(1 + e^{ikd})}{(\omega_0 - \Delta - k)[\omega_0 - k - i\Gamma(1 + e^{ikd})] - \Omega^2/4}, \\ u_e^\alpha(k) &= \frac{-\sqrt{\Gamma/\pi}(\omega_0 - \Delta - k)\cos kd/2}{(\omega_0 - \Delta - k)[\omega_0 - k - i\Gamma(1 + e^{ikd})] - \Omega^2/4}, \\ u_s^\alpha(k) &= \frac{\Omega/2\sqrt{\Gamma/\pi}\cos kd/2}{(\omega_0 - \Delta - k)[\omega_0 - k - i\Gamma(1 + e^{ikd})] - \Omega^2/4}. \end{aligned} \quad (30)$$

In order to construct the two-photon scattering wavefunction, we also employ the LS equation as stated above, in which the atomic operators are replaced by bosonic operators. To satisfy the level statistics, an additional on-site repulsion  $U$  must be introduced and assumed to

be infinite at the end. For a three-level atom, besides repulsion for each upper level, an additional term must be included in order that the double occupancy can be also fully ruled out. Here the repulsion operator  $\tilde{V}$  is

$$\tilde{V} = \frac{U}{2} \left( \hat{b}_e^\dagger \hat{b}_e^\dagger \hat{b}_e \hat{b}_e + \hat{b}_s^\dagger \hat{b}_s^\dagger \hat{b}_s \hat{b}_s + 2\hat{b}_e^\dagger \hat{b}_e \hat{b}_s^\dagger \hat{b}_s \right), \quad (31)$$

where the coefficient of the last term is chosen for convenience, and any coefficient would be cancelled out after taking  $U \rightarrow \infty$  [48]. Once a proper on-site interaction  $\tilde{V}$  is introduced, it is possible to calculate the two-photon wavefunction  $|\psi_2\rangle$  following the preceding steps. Consequently, the two-photon interacting eigenstate in the coordinate representation in the  $U \rightarrow \infty$  limit takes the form

$$\begin{aligned} {}_{\alpha'_1 \alpha'_2} \langle x_1 x_2 | \psi_2(k_1, k_2) \rangle_{\alpha_1 \alpha_2} &= {}_{\alpha'_1 \alpha'_2} \langle x_1 x_2 | \phi_2(k_1, k_2) \rangle_{\alpha_1 \alpha_2} \\ &\quad - \sum_{i, j=1}^3 G_i^{\alpha'_1 \alpha'_2}(x_1, x_2) (G^{-1})_{ij} \langle j | \phi_2(k_1, k_2) \rangle_{\alpha_1 \alpha_2}, \end{aligned} \quad (32)$$

in which we denote  $|1\rangle = |d_e d_e\rangle$ ,  $|2\rangle = |d_e d_s\rangle$  and  $|3\rangle = |d_s d_s\rangle$  for simplicity. The elements of Green functions are

$$\begin{aligned} G_i^{\alpha_1 \alpha_2}(x_1, x_2) &= {}_{\alpha_1 \alpha_2} \langle x_1 x_2 | G^R(E) | i \rangle \\ &= \sum_{\alpha'_1, \alpha'_2} \iint dk_1 dk_2 \frac{{}_{\alpha_1 \alpha_2} \langle x_1 x_2 | \phi_2(k_1, k_2) \rangle_{\alpha'_1 \alpha'_2} \langle \phi_2(k_1, k_2) | i \rangle}{E - k_1 - k_2 + i0^+}, \\ G_{ij} &= \langle i | G^R(E) | j \rangle = \\ &\quad \sum_{\alpha_1 \alpha_2} \iint dk_1 dk_2 \frac{\langle i | \phi_2(k_1, k_2) \rangle_{\alpha_1 \alpha_2} \langle \phi_2(k_1, k_2) | j \rangle}{E - k_1 - k_2 + i0^+}, \\ G^{-1} &= \begin{pmatrix} G_{11} & G_{12} & G_{13} \\ G_{21} & G_{22} & G_{23} \\ G_{31} & G_{32} & G_{33} \end{pmatrix}^{-1}, \end{aligned} \quad (33)$$

with the use of relations

$$\begin{aligned} \langle 1 | \phi_2(k_1, k_2) \rangle_{\alpha_1 \alpha_2} &= u_e^{\alpha_1}(k_1)u_e^{\alpha_2}(k_2), \\ \langle 2 | \phi_2(k_1, k_2) \rangle_{\alpha_1 \alpha_2} &= \frac{1}{2} [u_e^{\alpha_1}(k_1)u_s^{\alpha_2}(k_2) \\ &\quad + u_e^{\alpha_1}(k_2)u_s^{\alpha_2}(k_1)], \\ \langle 3 | \phi_2(k_1, k_2) \rangle_{\alpha_1 \alpha_2} &= u_s^{\alpha_1}(k_1)u_s^{\alpha_2}(k_2), \\ {}_{\alpha'_1 \alpha'_2} \langle x_1 x_2 | \phi_2(k_1, k_2) \rangle_{\alpha_1 \alpha_2} &= \frac{1}{2} [\phi_{\alpha'_1}^{\alpha_1}(k_1, x_1)\phi_{\alpha'_2}^{\alpha_2}(k_2, x_2) \\ &\quad + \phi_{\alpha'_1}^{\alpha_2}(k_2, x_1)\phi_{\alpha'_2}^{\alpha_1}(k_1, x_2)]. \end{aligned} \quad (34)$$

We also assume wavevector  $k$  in the accumulated phase shift as a constant  $k_0$  under the Markovian approximation, and denote  $k_0 d = \vartheta$ . Then by using the conventional contour integral techniques to get the double integral, we can obtain

$$\begin{aligned}
G_{11} &= \frac{16\Gamma^2 \cos^4 \frac{\vartheta}{2}}{(\lambda_1 - \lambda_2)^2} \left[ \frac{(\lambda_1 - \omega_0 + \Delta)^4}{f_1(\lambda_1, \lambda_2)} - \frac{(\lambda_1 - \omega_0 + \Delta)^2(\lambda_2 - \omega_0 + \Delta)^2}{f_2(\lambda_1, \lambda_2)} + \lambda_1 \leftrightarrow \lambda_2 \right], \\
G_{22} &= \frac{4\Gamma^2 \Omega^2 \cos^4 \frac{\vartheta}{2}}{(\lambda_1 - \lambda_2)^2} \left[ \frac{(\lambda_1 - \omega_0 + \Delta)^2}{f_1(\lambda_1, \lambda_2)} - \frac{(\lambda_1 + \lambda_2 - 2\omega_0 + 2\Delta)^2}{4f_2(\lambda_1, \lambda_2)} + \lambda_1 \leftrightarrow \lambda_2 \right], \\
G_{33} &= \frac{\Omega^4 \Gamma^2 \cos^4 \frac{\vartheta}{2}}{(\lambda_1 - \lambda_2)^2} \left[ \frac{1}{f_1(\lambda_1, \lambda_2)} - \frac{1}{f_2(\lambda_1, \lambda_2)} + \lambda_1 \leftrightarrow \lambda_2 \right], \\
G_{12} &= \frac{8\Omega\Gamma^2 \cos^4 \frac{\vartheta}{2}}{(\lambda_1 - \lambda_2)^2} \left[ \frac{(\lambda_1 - \omega_0 + \Delta)^3}{f_1(\lambda_1, \lambda_2)} - \frac{(\lambda_1 - \omega_0 + \Delta)^2(\lambda_2 - \omega_0 + \Delta)}{f_2(\lambda_1, \lambda_2)} + \lambda_1 \leftrightarrow \lambda_2 \right], \\
G_{13} &= \frac{4\Omega^2 \Gamma^2 \cos^4 \frac{\vartheta}{2}}{(\lambda_1 - \lambda_2)^2} \left[ \frac{(\lambda_1 - \omega_0 + \Delta)^2}{f_1(\lambda_1, \lambda_2)} - \frac{(\lambda_1 - \omega_0 + \Delta)(\lambda_2 - \omega_0 + \Delta)}{f_2(\lambda_1, \lambda_2)} + \lambda_1 \leftrightarrow \lambda_2 \right], \\
G_{23} &= \frac{2\Omega^3 \Gamma^2 \cos^4 \frac{\vartheta}{2}}{(\lambda_1 - \lambda_2)^2} \left[ \frac{(\lambda_1 - \omega_0 + \Delta)}{f_1(\lambda_1, \lambda_2)} - \frac{(\lambda_1 - \omega_0 + \Delta)}{f_2(\lambda_1, \lambda_2)} + \lambda_1 \leftrightarrow \lambda_2 \right], \\
G_{21} &= G_{12}, \quad G_{31} = G_{13}, \quad G_{32} = G_{23}, \\
G_1^{RR}(x_1, x_2) &= \frac{2\Gamma \cos^2 \frac{\vartheta}{2}}{\lambda_1 - \lambda_2} \left[ \frac{(\lambda_1 - \omega_0 + \Delta)(\lambda_1 + \omega_0 - \Delta - E)}{(2\lambda_1 - E)(\lambda_1 + \lambda_2 - E)} e^{iEx_2 - i\lambda_1 t} - \lambda_1 \leftrightarrow \lambda_2 \right], \\
G_2^{RR}(x_1, x_2) &= \frac{\Omega\Gamma \cos^2 \frac{\vartheta}{2}}{2(\lambda_1 - \lambda_2)} \left[ \frac{2\omega_0 - 2\Delta - E}{(2\lambda_1 - E)(\lambda_1 + \lambda_2 - E)} e^{iEx_2 - i\lambda_1 t} - \lambda_1 \leftrightarrow \lambda_2 \right], \\
G_3^{RR}(x_1, x_2) &= -\frac{\Omega^2 \Gamma \cos^2 \frac{\vartheta}{2}}{2(\lambda_1 - \lambda_2)} \left[ \frac{1}{(2\lambda_1 - E)(\lambda_1 + \lambda_2 - E)} e^{iEx_2 - i\lambda_1 t} - \lambda_1 \leftrightarrow \lambda_2 \right], \tag{35}
\end{aligned}$$

where

$$\begin{aligned}
f_1(\lambda_1, \lambda_2) &= (2\lambda_1 - E)(\lambda_1 - \lambda_1^*)^2(\lambda_1 - \lambda_2^*)^2, \\
f_2(\lambda_1, \lambda_2) &= (E - \lambda_1 - \lambda_2)(\lambda_1 - \lambda_1^*)(\lambda_2 - \lambda_2^*)|\lambda_1 - \lambda_2^*|^2, \\
\lambda_1 &= \frac{1}{2} \left[ 2\omega_0 - \Delta - i\Gamma' + \sqrt{(-\Delta + i\Gamma')^2 + \Omega^2} \right], \\
\lambda_2 &= \frac{1}{2} \left[ 2\omega_0 - \Delta - i\Gamma' - \sqrt{(-\Delta + i\Gamma')^2 + \Omega^2} \right], \tag{36}
\end{aligned}$$

with  $\Gamma' = \Gamma(1 + e^{i\vartheta})$ .

During the contour integrations,  $x_1 > d/2$ ,  $x_2 > d/2$ , and  $x = x_1 - x_2$ ,  $x_c = (x_1 + x_2)/2$  are used. It can also be proved that  $G_i^{LL}(-x_1, -x_2) = G_i^{RL}(x_1, -x_2) = G_i^{LR}(-x_1, x_2) = G_i^{RR}(x_1, x_2)$  ( $i = 1, 2, 3$ ) due to the parity symmetry. The interacting two-photon eigenstate becomes

$$\begin{aligned}
&|\psi_2(k_1, k_2)\rangle_{RR} = \\
&\iint dx_1 dx_2 f_{RR}^{(\Lambda)}(x_1, x_2) \frac{1}{\sqrt{2}} \hat{a}_R^\dagger(x_1) \hat{a}_R^\dagger(x_2) |0\rangle \\
&+ \iint dx_1 dx_2 f_{LL}^{(\Lambda)}(x_1, x_2) \frac{1}{\sqrt{2}} \hat{a}_L^\dagger(x_1) \hat{a}_L^\dagger(x_2) |0\rangle \\
&+ \iint dx_1 dx_2 f_{RL}^{(\Lambda)}(x_1, x_2) \hat{a}_R^\dagger(x_1) \hat{a}_L^\dagger(x_2) |0\rangle. \tag{37}
\end{aligned}$$

The coefficients can be written as the sum of plane-wave and bound-state terms

$$\begin{aligned}
f_{RR}^{(\Lambda)}(x_1, x_2) &= e^{iEx_c} \frac{\sqrt{2}}{2\pi} \left[ t_2(k_1) t_2(k_2) \cos \Delta_1 x + B_{k_1, k_2}^{(2)}(x) \right], \\
f_{LL}^{(\Lambda)}(x_1, x_2) &= e^{-iEx_c} \frac{\sqrt{2}}{2\pi} \left[ r_1(k_1) r_1(k_2) \cos \Delta_1 x + B_{k_1, k_2}^{(2)}(x) \right], \\
f_{RL}^{(\Lambda)}(x_1, x_2) &= \frac{e^{iEx/2}}{2\pi} \left[ t_2(k_1) r_1(k_2) e^{2i\Delta_1 x_c} \right. \\
&\quad \left. + r_1(k_1) t_2(k_2) e^{-2i\Delta_1 x_c} + 2B_{k_1, k_2}^{(2)}(x_c) \right]. \tag{38}
\end{aligned}$$

The bound-state term  $B_{k_1, k_2}^{(2)}(x)$  at the resonance, i.e.,  $\Delta = 0$ , is

$$\begin{aligned}
B_{k_1, k_2}^{(2)}(x) &= (1 + \cos \vartheta)^2 \Gamma^2 e^{i(E/2 - \omega_0)|x| - \Gamma' |x|/2} \\
&\times \left\{ \frac{(k_1 - \omega_0)(k_2 - \omega_0) \cos(\sqrt{\Omega^2 - \Gamma'^2} \frac{|x|}{2})}{[(k_1 - \omega_0)(k_1 - \omega_0 + i\Gamma') - \Omega^2/4][(k_2 - \omega_0)(k_2 - \omega_0 + i\Gamma') - \Omega^2/4]} \right. \\
&- \left. \frac{[\Gamma'(k_1 - \omega_0)(k_2 - \omega_0) + i(k_1 + k_2 - 2\omega_0)\Omega^2/4] \sin(\sqrt{\Omega^2 - \Gamma'^2} \frac{|x|}{2})}{\sqrt{\Omega^2 - \Gamma'^2}[(k_1 - \omega_0)(k_1 - \omega_0 + i\Gamma') - \Omega^2/4][(k_2 - \omega_0)(k_2 - \omega_0 + i\Gamma') - \Omega^2/4]} \right\} \quad (39)
\end{aligned}$$

with  $\Gamma' = \Gamma(1 + e^{i\vartheta})$ . If  $\Omega = 0$ , these coefficients can be reduced to the same form as the two-level giant atom derived above. In the following discussion the identical incident photons are assumed, i.e.,  $k_1 = k_2 = E/2$ , where  $E$  is the total energy.

### A. Incoherent power spectrum and two-photon correlation function

#### 1. Incoherent power spectrum

According to the preceding discussion of the two-level giant atom system, the total incoherent power spectrum can be used as a measure of photon-photon correlation because it is derived from the correlated bound state. For the three-level giant atom, the exact derivation of total incoherent power spectrum  $F(k)$  is presented in the appendix, which is

$$\begin{aligned}
F(k) &= \frac{-32(1 + \cos \vartheta)^4 \Gamma^4 (E/2 - \omega_0)^2 / \pi}{|(E/2 - \omega_0 + \gamma_+)(E/2 - \omega_0 + \gamma_-)|^2} \text{Im} \left\{ \frac{1}{(E - 2\omega_0 + i\Gamma') \sqrt{\Omega^2 - \Gamma'^2}} \right. \\
&\times \left. \left[ \frac{[\gamma_+(E - 2\omega_0 + \gamma_+) + \Omega^2/4]^2 / [(\gamma_+^* - \gamma_+)(\gamma_-^* - \gamma_+)]}{(E - 2\omega_0 + 2\gamma_+)(E - 2\omega_0 + \gamma_+ + \gamma_+^*)(E - 2\omega_0 + \gamma_+ + \gamma_-^*)} - (+ \leftrightarrow -) \right] \right\}, \quad (40)
\end{aligned}$$

with  $\gamma_{\pm} = \pm \frac{1}{2} \sqrt{\Omega^2 - \Gamma'^2} + \frac{i}{2} \Gamma'$ , and  $\text{Im}\{\dots\}$  means the imaginary part. The result is numerically shown in Fig. 5. At the perfect electromagnetically-induced transparency (EIT) window, i.e.,  $k_1 = k_2 = \omega_0$ ,  $F(k)$  equals to zero, which reveals that all the photons are scattered coherently, and bound state is not formed in the wavefunction. This can also be verified by the expression of bound-state term in Eq. (39), which becomes zero when  $k_1 = k_2 = \omega_0$ . This is consistent with the idea that photon-photon correlation and incoherent scattering are related. Additionally,  $F(k_{\text{in}} = \omega_0) = 0$  at the perfect transparency is irrelevant to the phase shift  $\vartheta$ , and even the number of identical atoms coupled to the waveguide [48]. This phenomenon has been termed as fluorescence quenching [29, 49].

The large value of  $F(k)$  indicates a significant photon-photon correlation, which is supported by the relationship between the incoherent power spectrum and photon-photon correlation. In Fig. 5 the peak value of  $F(k)$  of three-level giant atom is substantially greater than that of the two-level giant atom. This indicates that photon-photon correlation is produced more efficiently by the

three-level giant atom. Additionally, if  $\vartheta = 0$ , the shape of  $F(k)$  is symmetry, and analogous to that of single-point coupling [48]. However, the magnitude of incoherent scattering substantially increases for the other phase shifts, such as  $\vartheta = 0.5\pi$  and  $\vartheta = 0.75\pi$ , and the line shape changes from symmetry to asymmetry. This can be explained by the asymmetric pole structure. The poles refers to  $\lambda_1$  and  $\lambda_2$  in Eq. (36). For  $\vartheta = 0$ , the poles' real parts are symmetric with respect to  $\omega_0$ , while for  $\vartheta = 0.5\pi$  and  $\vartheta = 0.75\pi$ , they become asymmetric. In addition, the hight of the peak is inversely proportional to its width, which is defined by the imaginary part of the pole. For example, when  $\vartheta = 0.5\pi$ , the two poles are  $\omega_0 + 1.03 - 0.97i$  and  $\omega_0 - 0.032 - 0.03i$ . As a result, the main peak is located at  $\omega_0 - 0.032$  while the other peak is ignorable for the large imaginary part. When  $\vartheta = 0.75\pi$ , the two poles are  $\omega_0 + 0.78 - 0.27i$  and  $\omega_0 - 0.072 - 0.025i$ , so the main peak is located at  $\omega_0 - 0.072$ . The height of peak is higher because the imaginary part is smaller. At the same time, the other peak is located at the  $\omega_0 + 0.78$  with a smaller height due to its a little larger imaginary part.

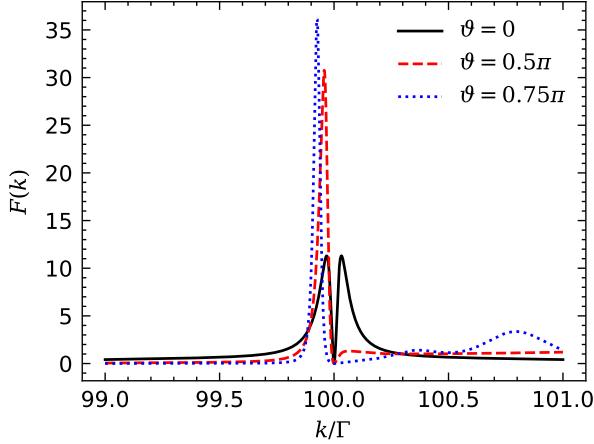


FIG. 5. The total incoherent power spectrum  $F(k)$  of the three-level giant atom as a function of the incident frequency  $k$  with different values of  $\vartheta$ . The other parameters are  $\omega_0 = 100\Gamma$ ,  $k_1 = k_2 = k = E/2$  and  $\Omega = \Gamma/2$ .

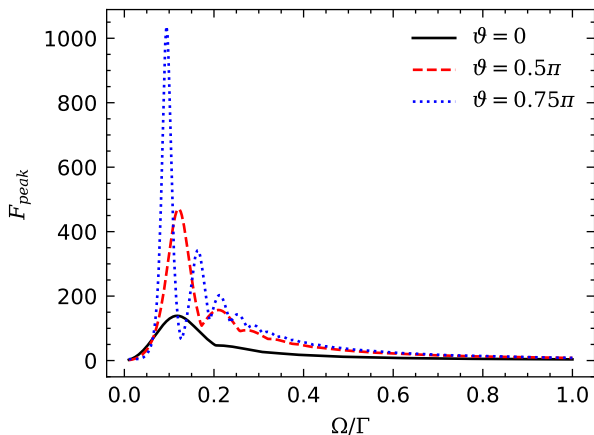


FIG. 6. The peak value of total incoherent power spectrum  $F_{\text{peak}}$  of the three-level giant atom as a function of Rabi frequency  $\Omega$  with different values of  $\vartheta$ . The other parameters are  $\omega_0 = 100\Gamma$ ,  $k_1 = k_2 = k = E/2$ .

The effect of increasing the Rabi frequency  $\Omega$  is very similar to that of a single three-level atom. The peak value in  $F(k)$  become smaller with the increased Rabi frequency as shown in Fig. 6. Therefore, the strong Rabi frequency will prevent the photon-photon correlation, providing a relatively simple and structureless effects, which may be preferable in some circumstance [47].

## 2. The second-order correlation function

Likewise, the second-order correlation functions are employed to investigate the photon-photon correlation of the transmitted and reflected field ( $x_1 > d/2$ ,  $x_2 > d/2$ , and  $x = x_2 - x_1$ ) in the system of three-level giant atom,

which are defined by

$$g_R^{(2)}(x) = \frac{2\pi^2 |f_{RR}^{(\Lambda)}(x_1, x_2)|^2}{|t_2(k_1)|^2 |t_2(k_2)|^2},$$

$$g_L^{(2)}(x) = \frac{2\pi^2 |f_{LL}^{(\Lambda)}(x_1, x_2)|^2}{|r_1(k_1)|^2 |r_1(k_2)|^2}, \quad (41)$$

for the weak incident field. From the definition, it can be proved that at the perfect EIT window, i.e.,  $k_1 = k_2 = \omega_0$ ,  $g_{R/L}^{(2)}(x) = 1$  because the bound term in Eq. (39) is equal to zero. All of the photons are scattered coherently, without structured correlation effects, which is consistent with the zero of  $F(k)$ . Actually, the generation of strong photon interactions indicated by peak value of  $F(k)$  appears slightly away from EIT conditions [47]. Thus,  $\omega_0 - E/2 = 0.05\Gamma$  is chosen in the numerical plot of  $g_{R/L}^{(2)}(x)$  in Fig. 7.

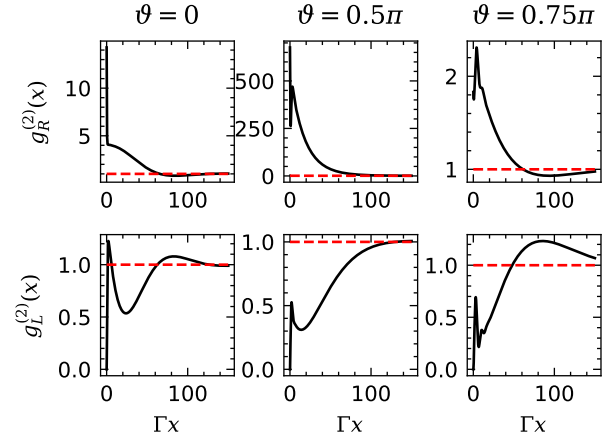


FIG. 7. Second-order correlation function  $g_R^{(2)}(x)$  in the system of three-level giant atom (transmitted photons, first row) and  $g_L^{(2)}(x)$  (reflected photons, second row). First column is  $\vartheta = 0$ , second column is  $\vartheta = 0.5\pi$ , and third column is  $\vartheta = 0.75\pi$ . The dashed horizontal line refers to  $g^{(2)}(x) = 1$ . The other parameters are  $k_1 = k_2 = E/2$ ,  $\omega_0 - E/2 = 0.05\Gamma$ , and  $\Omega = \Gamma/2$ .

Initially at  $x = 0$ , the transmitted photons are bunched and the reflected photons are antibunched, similar to that of a single coupling point [48]. The initial value cannot be used to predict the overall photon-photon correlation, since the shape of  $g_{R/L}^{(2)}(x)$  is more complicated than that results from beating between different eigenfrequencies and incident frequency. In addition to the improved photon-photon correlation compared to the two-level atom, the correlation lasts for a longer distance. The long decay distance can be characterized by the smaller value of imaginary part of the poles. When  $\vartheta = 0$ , the decay time is on the time scale of  $8\Gamma/\Omega^2$ , which is longer than that of two-level atom with the use of the weak Rabi frequency  $\Omega$ . For  $\vartheta = 0.5\pi$  and  $\vartheta = 0.75\pi$ , the imaginary

parts becomes further smaller, the much longer distance correlation is achievable.

The experimental feasibility of efficient coupling between the giant quantum emitters and waveguides can be achieved by implementing both with superconducting qubits coupled either to microwave transmission lines [12, 13] or surface acoustic waves and cold atoms [50], respectively. For instance, the qubit coupled to the meandering transmission line is demonstrated in Ref. [12]. In the setup, giant qubits have a spontaneous dissipation rate  $\gamma_e/2\pi = 0.03$  MHz in comparison to  $\Gamma/2\pi \sim 3$  MHz. It is reasonable to neglect the spontaneous dissipation rate  $\gamma_e$  in our previous treatment. Furthermore, the  $\Lambda$ -configuration of a giant transmon coupled to a transmission line is also demonstrated in Ref. [13], and its characteristic phenomenon, i.e., EIT, is observed.

#### IV. CONCLUSIONS

In conclusion, we have used the LS method to show the two-photon scattering processes of two- and three-level giant atom coupled to a 1D waveguide, and focused on effects of the accumulated phase shift gained by photons traveling between coupling points. The multiple coupling points of giant atom give rise to interference effects that are not present in point-like atoms. Based on the analytical results of total incoherent power spectra and second-order correlation functions of scattered photons, we find that the phase shift can be used to improve strength and distance of photon-photon interactions. In the system of two-level giant atom, photon-photon interactions can be enhanced and the evolution of the second-order correlation exhibits an oscillation between bunching and anti-bunching. Compared to the two-level giant atom, the photon-photon correlation can be substantially increased in the system of the three-level giant atom. The photon-photon interactions and correlation distance can be further enhanced by tuning the accumulated phase shift between the two coupling points.

#### ACKNOWLEDGMENTS

This work was supported by the National Natural Science Foundation of China (under Grants No.1150403, 61505014, 12174140.)

#### Appendix A: Calculation of the incoherent power spectrum

##### 1. The two-level giant atom

The power spectrum or resonance fluorescence is defined by the Fourier transform of the first-order coherence

ence

$$S_\alpha(\omega) = \int dt e^{-i\omega t} \langle \psi_2 | \hat{a}_\alpha^\dagger(x_0) \hat{a}_\alpha(x_0 + t) | \psi_2 \rangle, (\alpha = R, L), \quad (A1)$$

where  $x_0$  is the position of detector that is far away from the scattering region. For example of  $\alpha = R$ , the first-order coherence in  $|\psi_2\rangle$  is

$$\langle \psi_2 | \hat{a}_R^\dagger(x_0) \hat{a}_R(x_0 + t) | \psi_2 \rangle = 2 \int dx' f_{RR}^*(x_0, x') f_{RR}(x_0 + t, x'), \quad (A2)$$

and under the condition of identical incident photons, i.e.,  $k_1 = k_2 = E/2$ ,

$$\begin{aligned} f_{RR}^*(x_0, x') f_{RR}(x_0 + t, x') = \\ \frac{e^{iEt/2}}{2\pi^2} \left[ |t_2(E/2)|^4 + t_2^2(E/2) B_{k_1, k_2}^*(x) \right. \\ \left. + t_2^{*2}(E/2) B_{k_1, k_2}(x - t) + B_{k_1, k_2}^*(x) B_{k_1, k_2}(x - t) \right], \end{aligned} \quad (A3)$$

with  $x = x' - x_0$ . Via substituting Eqs. (A2) and (A3) into Eq. (A1), the power spectrum can be divided into two parts,

$$S_R(\omega) = S_R^{\text{coherent}}(\omega) + S_R^{\text{incoherent}}(\omega), \quad (A4)$$

where the coherent part contains terms proportional to  $\delta(0)\delta(\omega - E/2)$  because delta-normalized plane waves are used, and the incoherent part is related to the correlation of the bound term

$$S_R^{\text{incoherent}}(\omega) = \frac{1}{\pi^2} \iint dt dx e^{i(E/2 - \omega)t} B_{k_1, k_2}^*(x) B_{k_1, k_2}(x - t). \quad (A5)$$

After the integration, the incoherent power spectrum becomes

$$\begin{aligned} S_R^{\text{incoherent}}(\omega) = \frac{4}{\pi^2} \\ \times \frac{\Gamma^4(1 + \cos \vartheta)^4}{|(E/2 - \omega_0 + i\Gamma')(E - \omega - \omega_0 + i\Gamma')(\omega - \omega_0 + i\Gamma')|^2}. \end{aligned} \quad (A6)$$

The total incoherent power spectrum is the sum of right and left-moving incoherent power spectra,

$$S^{\text{incoherent}}(\omega) = S_R^{\text{incoherent}}(\omega) + S_L^{\text{incoherent}}(\omega), \quad (A7)$$

and here it can prove that  $S_R^{\text{incoherent}}(\omega) = S_L^{\text{incoherent}}(\omega)$ . The total incoherent power can be used to measure the overall strength of photon-photon correlations to show the non-classical effects. The definition of incoherently scattered photon flux is

$$F(k) = \int d\omega S^{\text{incoherent}}(\omega), \quad (A8)$$

and via integrating over  $\omega$ , it becomes

$$F(k) = \frac{4\Gamma^3(1 + \cos \vartheta)^3}{\pi |E/2 - \omega_0 + i\Gamma'|^4}. \quad (A9)$$

## 2. The three-level giant atom

The incoherent power spectral of three-level giant atom can be calculated by following the same procedure as that of the two-level giant atom, which yields

$$S_R^{\text{incoherent}}(\omega) = \frac{4}{\pi^2} \frac{(1 + \cos \vartheta)^4 \Gamma^4 (E/2 - \omega_0)^2}{|(E/2 - \omega_0 + \gamma_+)(E/2 - \omega_0 + \gamma_-)(\omega - \omega_0 + \gamma_+)|^2} \times \frac{[(E - \omega - \omega_0)(\omega - \omega_0) - \Omega^2/4]^2}{|(\omega - \omega_0 + \gamma_-)(E - \omega - \omega_0 + \gamma_+)(E - \omega - \omega_0 + \gamma_-)|^2}, \quad (\text{A10})$$

where  $\gamma_{\pm} = \pm \frac{1}{2} \sqrt{\Omega^2 - \Gamma'^2} + \frac{i}{2} \Gamma'$ . By integrating over

the frequency  $\omega$ , the incoherently scattered photon flux  $F(k) = 2 \int d\omega S_R^{\text{incoherent}}(\omega)$  becomes

$$F(k) = \frac{-32(1 + \cos \vartheta)^4 \Gamma^4 (E/2 - \omega_0)^2 / \pi}{|(E/2 - \omega_0 + \gamma_+)(E/2 - \omega_0 + \gamma_-)|^2} \text{Im} \left\{ \frac{1}{(E - 2\omega_0 + i\Gamma') \sqrt{\Omega^2 - \Gamma'^2}} \times \left[ \frac{[\gamma_+(E - 2\omega_0 + \gamma_+) + \Omega^2/4]^2 / [(\gamma_+^* - \gamma_+)(\gamma_-^* - \gamma_+)]}{(E - 2\omega_0 + 2\gamma_+)(E - 2\omega_0 + \gamma_+ + \gamma_+^*)(E - 2\omega_0 + \gamma_+ + \gamma_-^*)} - (+ \leftrightarrow -) \right] \right\}. \quad (\text{A11})$$

---

[1] D. Roy, C. M. Wilson, and O. Firstenberg, Colloquium: Strongly interacting photons in one-dimensional continuum, *Rev. Mod. Phys.* **89**, 021001 (2017).

[2] X. Gu, A. F. Kockum, A. Miranowicz, Y.-X. Liu, and F. Nori, Microwave photonics with superconducting quantum circuits, *Physics Reports* **718-719**, 1 (2017).

[3] A. S. Sheremet, M. I. Petrov, I. V. Iorsh, A. V. Poshakinskiy, and A. N. Poddubny, Waveguide quantum electrodynamics: Collective radiance and photon-photon correlations, *Rev. Mod. Phys.* **95**, 015002 (2023).

[4] P. Forn-Díaz, J. J. García-Ripoll, B. Peropadre, J. L. Orgiazzi, M. A. Yurtalan, R. Belyansky, C. M. Wilson, and A. Lupascu, Ultrastrong coupling of a single artificial atom to an electromagnetic continuum in the nonperturbative regime, *Nature Physics* **13**, 39 (2017).

[5] D. E. Chang, V. Vuletić, and M. D. Lukin, Quantum nonlinear optics - Photon by photon, *Nature Photonics* **8**, 685 (2014).

[6] T. Shi, Y.-H. Wu, A. González-Tudela, and J. I. Cirac, Effective many-body hamiltonians of qubit-photon bound states, *New Journal of Physics* **20**, 105005 (2018).

[7] N. Fayard, L. Henriet, A. Asenjo-Garcia, and D. E. Chang, Many-body localization in waveguide quantum electrodynamics, *Phys. Rev. Res.* **3**, 033233 (2021).

[8] B. Kannan, A. Almanaky, Y. Sung, A. Di Paolo, D. A. Rower, J. Braumüller, A. Melville, B. M. Niedzielski, A. Karamlou, K. Serniak, A. Vepsäläinen, M. E. Schwartz, J. L. Yoder, R. Winik, J. I.-J. Wang, T. P. Orlando, S. Gustavsson, J. A. Grover, and W. D. Oliver, On-demand directional microwave photon emission using waveguide quantum electrodynamics, *Nature Physics* **19**, 394 (2023).

[9] A. González-Tudela, V. Paulisch, D. E. Chang, H. J. Kimble, and J. I. Cirac, Deterministic generation of arbitrary photonic states assisted by dissipation, *Phys. Rev. Lett.* **115**, 163603 (2015).

[10] P. Forn-Díaz, C. W. Warren, C. W. S. Chang, A. M. Vadiraj, and C. M. Wilson, On-demand microwave generator of shaped single photons, *Phys. Rev. Appl.* **8**, 054015 (2017).

[11] G. Andersson, B. Suri, L. Guo, T. Aref, and P. Delsing, Non-exponential decay of a giant artificial atom, *Nature Physics* **15**, 1123 (2019).

[12] B. Kannan, M. J. Ruckriegel, D. L. Campbell, A. Frisk Kockum, J. Braumüller, D. K. Kim, M. Kjaergaard, P. Krantz, A. Melville, B. M. Niedzielski, A. Vepsäläinen, R. Winik, J. L. Yoder, F. Nori, T. P. Orlando, S. Gustavsson, and W. D. Oliver, Waveguide quantum electrodynamics with superconducting artificial giant atoms, *Nature* **583**, 775 (2020).

[13] A. M. Vadiraj, A. Ask, T. G. McConkey, I. Nsanzineza, C. W. S. Chang, A. F. Kockum, and C. M. Wilson, Engineering the level structure of a giant artificial atom in waveguide quantum electrodynamics, *Phys. Rev. A* **103**,

023710 (2021).

[14] A. Frisk Kockum, P. Delsing, and G. Johansson, Designing frequency-dependent relaxation rates and lamb shifts for a giant artificial atom, *Phys. Rev. A* **90**, 013837 (2014).

[15] A. F. Kockum, G. Johansson, and F. Nori, Decoherence-free interaction between giant atoms in waveguide quantum electrodynamics, *Phys. Rev. Lett.* **120**, 140404 (2018).

[16] A. Carollo, D. Cilluffo, and F. Ciccarello, Mechanism of decoherence-free coupling between giant atoms, *Phys. Rev. Res.* **2**, 043184 (2020).

[17] S. Longhi, Photonic simulation of giant atom decay, *Opt Lett* **45**, 3017 (2020).

[18] S. Guo, Y. Wang, T. Purdy, and J. Taylor, Beyond spontaneous emission: Giant atom bounded in the continuum, *Phys. Rev. A* **102**, 033706 (2020).

[19] L. Guo, A. F. Kockum, F. Marquardt, and G. Johansson, Oscillating bound states for a giant atom, *Phys. Rev. Res.* **2**, 043014 (2020).

[20] J. T. Shen and S. Fan, Coherent photon transport from spontaneous emission in one-dimensional waveguides, *Opt Lett* **30**, 2001 (2005).

[21] J.-T. Shen and S. Fan, Coherent single photon transport in a one-dimensional waveguide coupled with superconducting quantum bits, *Phys. Rev. Lett.* **95**, 213001 (2005).

[22] T. Shi and C. P. Sun, Lehmann-symanzik-zimmermann reduction approach to multiphoton scattering in coupled-resonator arrays, *Phys. Rev. B* **79**, 205111 (2009).

[23] T. Shi, S. Fan, and C. P. Sun, Two-photon transport in a waveguide coupled to a cavity in a two-level system, *Phys. Rev. A* **84**, 063803 (2011).

[24] J.-Q. Liao and C. K. Law, Correlated two-photon transport in a one-dimensional waveguide side-coupled to a nonlinear cavity, *Phys. Rev. A* **82**, 053836 (2010).

[25] J.-Q. Liao and C. K. Law, Correlated two-photon scattering in cavity optomechanics, *Phys. Rev. A* **87**, 043809 (2013).

[26] H. Zheng and H. U. Baranger, Persistent quantum beats and long-distance entanglement from waveguide-mediated interactions, *Phys. Rev. Lett.* **110**, 113601 (2013).

[27] Y.-L. L. Fang, H. Zheng, and H. U. Baranger, One-dimensional waveguide coupled to multiple qubits: photon-photon correlations, *EPJ Quantum Technology* **1**, 3 (2014).

[28] S. Fan, i. m. c. E. Kocabas, and J.-T. Shen, Input-output formalism for few-photon transport in one-dimensional nanophotonic waveguides coupled to a qubit, *Phys. Rev. A* **82**, 063821 (2010).

[29] E. Rephaeli, i. m. c. E. Kocabas, and S. Fan, Few-photon transport in a waveguide coupled to a pair of colocated two-level atoms, *Phys. Rev. A* **84**, 063832 (2011).

[30] D. L. Hurst and P. Kok, Analytic few-photon scattering in waveguide qed, *Phys. Rev. A* **97**, 043850 (2018).

[31] W. Zhao and Z. Wang, Single-photon scattering and bound states in an atom-waveguide system with two or multiple coupling points, *Phys. Rev. A* **101**, 053855 (2020).

[32] S. L. Feng and W. Z. Jia, Manipulating single-photon transport in a waveguide-qed structure containing two giant atoms, *Phys. Rev. A* **104**, 063712 (2021).

[33] L. Du, Y.-T. Chen, and Y. Li, Nonreciprocal frequency conversion with chiral  $\Lambda$ -type atoms, *Phys. Rev. Res.* **3**, 043226 (2021).

[34] X.-L. Yin, Y.-H. Liu, J.-F. Huang, and J.-Q. Liao, Single-photon scattering in a giant-molecule waveguide-qed system, *Phys. Rev. A* **106**, 013715 (2022).

[35] H. Zheng, D. J. Gauthier, and H. U. Baranger, Strongly correlated photons generated by coupling a three- or four-level system to a waveguide, *Phys. Rev. A* **85**, 043832 (2012).

[36] Z. Yi, H. Huang, Y. Yan, L. Sun, and W. Gu, Correlated two-photon scattering in a 1d waveguide coupled to an n-type four-level emitter, *Annalen der Physik* **535**, 2200512 (2023), <https://onlinelibrary.wiley.com/doi/pdf/10.1002/andp.202200512>.

[37] W.-j. Gu, L. Wang, Z. Yi, and L.-h. Sun, Generation of nonreciprocal single photons in the chiral waveguide-cavity-emitter system, *Phys. Rev. A* **106**, 043722 (2022).

[38] J. Tang, Y. Wu, Z. Wang, H. Sun, L. Tang, H. Zhang, T. Li, Y. Lu, M. Xiao, and K. Xia, Vacuum-induced surface-acoustic-wave phonon blockade, *Phys. Rev. A* **101**, 053802 (2020).

[39] E. S. Redchenko, A. V. Poshakinskiy, R. Sett, M. Žemlička, A. N. Poddubny, and J. M. Fink, Tunable directional photon scattering from a pair of superconducting qubits, *Nature Communications* **14**, 2998 (2023).

[40] I.-C. Hoi, T. Palomaki, J. Lindkvist, G. Johansson, P. Delsing, and C. M. Wilson, Generation of nonclassical microwave states using an artificial atom in 1d open space, *Phys. Rev. Lett.* **108**, 263601 (2012).

[41] S. Xu, E. Rephaeli, and S. Fan, Analytic properties of two-photon scattering matrix in integrated quantum systems determined by the cluster decomposition principle, *Phys. Rev. Lett.* **111**, 223602 (2013).

[42] W. Zhao, Y. Zhang, and Z. Wang, Phase-modulated autler-townes splitting in a giant-atom system within waveguide qed, *Frontiers of Physics* **17**, 42506 (2022).

[43] P. Longo, P. Schmitteckert, and K. Busch, Few-photon transport in low-dimensional systems: Interaction-induced radiation trapping, *Phys. Rev. Lett.* **104**, 023602 (2010).

[44] J.-T. Shen and S. Fan, Strongly correlated multiparticle transport in one dimension through a quantum impurity, *Phys. Rev. A* **76**, 062709 (2007).

[45] Y.-L. L. Fang and H. U. Baranger, Waveguide qed: Power spectra and correlations of two photons scattered off multiple distant qubits and a mirror, *Phys. Rev. A* **91**, 053845 (2015).

[46] R. Loudon, *The quantum theory of light* (Oxford University Press, 2000).

[47] D. Roy and N. Bondyopadhyaya, Statistics of scattered photons from a driven three-level emitter in a one-dimensional open space, *Phys. Rev. A* **89**, 043806 (2014).

[48] Y.-L. L. Fang and H. U. Baranger, Photon correlations generated by inelastic scattering in a one-dimensional waveguide coupled to three-level systems, *Physica E: Low-dimensional Systems and Nanostructures* **78**, 92 (2016).

[49] P. Zhou and S. Swain, Ultranarrow spectral lines via quantum interference, *Phys. Rev. Lett.* **77**, 3995 (1996).

[50] A. Frisk Kockum, Quantum optics with giant atoms—the first five years, in *International Symposium on Mathematics, Quantum Theory, and Cryptography*, edited by T. Takagi, M. Wakayama, K. Tanaka, N. Kunihiro, K. Kimoto, and Y. Ikematsu (Springer Singapore, Singapore,

2021) pp. 125–146.